International Journal of Thermophysics, Vol. 26, No. 5, September 2005 (© 2005)
DOI: 10.1007/s10765-005-8089-2

High-Pressure Viscosity Measurements for the Ethanol + Toluene Binary System

C. K. Zéberg-Mikkelsen,[1] A. Baylaucq,[2] G. Watson,[2] and C. Boned[2,3]

Received April 21, 2005

The viscosity of the ethanol + toluene binary system has been measured with a falling-body viscometer for seven compositions as well as for the pure ethanol in the temperature range from 293.15 to 353.15 K and up to 100 MPa with an experimental uncertainty of 2%. At 0.1 MPa the viscosity has been measured with a classical capillary viscometer (Ubbelohde) with an uncertainty of 1%. A total of 209 experimental measurements have been obtained for this binary system, which reveals a non-monotonic behavior of the viscosity as a function of the composition, with a minimum. The viscosity behavior of this binary system is interpreted as the result of changes in the free volume, and the breaking or weakening of hydrogen bonds. The excess activation energy for viscous flow of the mixtures is negative with a maximum absolute value of $335\,J \cdot mol^{-1}$, indicating that this binary system is a very weakly interacting system showing a negative deviation from ideality. The viscosity of this binary system is represented by the Grunberg–Nissan and the Katti–Chaudhri mixing laws with an overall uncertainty of 12% and 8%, respectively. The viscosity of methanol (23 point) has also been measured in order to verify the calibration of the falling-body viscometer within the considered *T, P* range.

KEY WORDS: ethanol; high pressure; hydrocarbon; methanol; measurements; viscosity.

[1] Center for Phase Equilibria and Separation Processes (IVCSEP), Department of Chemical Engineering, Technical University of Denmark, Building 229, 2800 Lyngby, Denmark.
[2] Laboratoire des Fluides Complexes, Faculté des Sciences et Techniques, UMR CNRS 5150, Université de Pau, BP 1155, 64013 Pau Cedex, France.
[3] To whom correspondence should be addressed. E-mail: christian.boned@univ-pau.fr

1. INTRODUCTION

Ethanol is a widely used compound in many industrial applications, such as solvent in paints or pharmaceuticals, and in the manufacturing of acetic acid, ether, or high-molecular weight chemicals. In recent years, ethanol has become of interest as an additive to gasoline instead of the commonly used compound methyl *tert*-butyl ether (MTBE), which is found to have some environmental side effects, e.g., penetrating through the soil and polluting the groundwater, making it undesirable for human consumption. As a consequence, ethanol is now, e.g., in the U.S.A., added to gasoline (gasohol) in proportions up to 10 vol.%. As discussed by French and Malone [1], the addition of ethanol to gasoline affects the production, storage, distribution, and use of the obtained gasoline, because the physical properties are changed and complex thermodynamic behaviors are encountered.

Since aromatic hydrocarbons are important constituents in petroleum and gasoline fluids, complex fluid behaviors may be encountered when polar compounds, such as ethanol, are added to these fluids due to weak intermolecular interactions between the aromatic hydrocarbons and the alcohol. This is the result of an electron donor–acceptor type of interactions between the π electrons of the aromatic compounds and the hydroxyl group of the alcohol. The evidence for the ability of aromatic compounds to act as electron donors has been experimentally and theoretically studied by several researchers using different IR spectroscopic methods or molecular orbital theory, see, e.g., Refs. 2–5. In order to study the behavior of ethanol + petroleum fluids under various operating conditions, experimental property measurements of simplified mixtures can provide valuable information about their behavior both from a fundamental as well as an applied point of view. Although the viscosity is an important fluid property required in various engineering disciplines, only a few experimental viscosity studies under pressure have previously been performed on systems involving alcohols and hydrocarbons [6, 7].

Recently, the density of the ethanol + toluene binary system [8] has been measured in the temperature range from 283.15 to 353.15 K and up to 45 MPa, showing that molecular interactions occur within the mixture. In order to study the viscosity behavior of this system as well as to provide more experimental viscosity data for asymmetrical systems involving hydrocarbons and industrially important alcohols, such as ethanol, an extensive experimental study of the viscosity for the asymmetrical ethanol + toluene binary system has been performed up to 100 MPa in the temperature range from 293.15 to 353.15 K. The

experimental viscosity data are further used in a study of the excess activation energy for viscous flow, ΔE_a, and to evaluate the performance of the Grunberg and Nissan [9] and Katti and Chaudhri [10] mixing laws.

2. EXPERIMENTAL TECHNIQUES

The dynamic viscosity η under pressure has been measured using a falling-body viscometer. This viscometer is of the type designed by Daugé et al. [11] in order to measure the liquid and dense phase viscosity of fluids with a low viscosity that are not in the single liquid phase at atmospheric pressure. The viscometer consists of two high-pressure cells, a measuring cell and a piston cell, which are connected by a capillary tube and a valve, see Fig. 1 in Ref. 11. A detailed description of the measuring tube is given in Ref. 11. The piston cell is connected to a pneumatic oil pump, which is used to pressurize the viscometer. The pressure of the sample within the viscometer is measured by a HBM-P3M manometer connected directly to the tube between the two cells, ensuring a measure of the real pressure of the sample. The pressure is measured with an uncertainty of 0.1 MPa. The temperature is measured inside the measuring cell by a Pt100 probe connected to a classical AOIP thermometer with an uncertainty of 0.5 K. The temperature of the sample in the measuring cell and the piston cell is controlled by a circulating fluid supplied by an external thermostatic bath. The viscometer is placed in an automated air-pulsed thermal regulator box in order to ensure a homogeneous temperature surrounding the system.

In the case of fluids, which are liquids at atmospheric pressure, the filling operation of the viscometer is simplified compared to the procedure described in Ref. 11. The viscometer is filled in the following way: after the piston is moved to the top of the cell, the piston cell and the measuring cell are brought under vacuum using a vacuum pump through the double valve in order to allow the filling of the viscometer by gravity. Then the valve connecting the capillary tubes between the measuring tube and the piston cell is closed and a filling tube with a funnel is connected to the double valve. After the sample is filled into the filling tube and the funnel, free of any air bubbles, the double valve is opened allowing a complete filling of the piston cell. Then the valve connecting the capillary tubes between the two cells is opened, and the measuring cell is filled.

The basic principle of the falling-body viscometer is that a sinker falls through a fluid of unknown viscosity under a given temperature and pressure (T, P) condition. It has been emphasized by Daugé et al. [11] that, for this type of viscometer and for fluids with a low viscosity, a work-

ing equation of the functional form: $\eta(T, P) = f[(\rho_s - \rho_L)\Delta\tau]$ should be used. This working equation relates the dynamic viscosity to the difference between the density of the sinker ρ_s and of the fluid ρ_L, and the falling time between two detection sensors $\Delta\tau$, when the velocity of the sinker is constant. For fluids with a dynamic viscosity less than 0.3 mPa · s, such as methane, Daugé et al. [11] used a second order polynomial in $(\rho_s - \rho_L)\Delta\tau$, which implies the requirement of three reference fluids in order to perform the calibration of the viscometer. However, in this work the lowest viscosity is higher than 0.3 mPa · s, and consequently, it was found appropriate to use a linear relation for the working equation as follows:

$$\eta(T, P) = K_a(T, P) + K_b(T, P)(\rho_s - \rho_L)\Delta\tau \quad (1)$$

which relates the dynamic viscosity to two apparatus constants, K_a and K_b. A similar working equation has recently been used by Pensado et al. [12].

The sinker used in this work is a solid stainless steel cylinder with hemispherical ends and a density of 7720 kg · m^{-3}. The sinker is designed with a ratio between its diameter and the tube diameter greater than 0.98, which is substantially above the recommended value of 0.93 in order to ensure a concentric fall and to minimize eccentricity effects [13–15]. Since the density of the sinker is about nine times higher than the density of the fluids considered in this work, an error in the fluid density of 0.1% results in an error of about 1/7000 in the viscosity. In this work, $\Delta\tau$ corresponds to the average value of six measurements of the falling time at thermal and mechanical equilibrium with a reproducibility of 0.5%.

The calibration of the viscometer has been performed with toluene and *n*-decane. The apparatus constants $K_a(T, P)$ and $K_b(T, P)$ are determined at each considered (T, P) condition by plotting the reference viscosities of the two calibrating fluids as a function of $(\rho_s - \rho_L)\Delta\tau$. In this work, the required reference viscosity and density data for toluene have been estimated by the correlations given for the viscosity and density by Assael et al. [16]. The reported uncertainty for the calculated density and viscosity values is 0.03% and 2%, respectively. For *n*-decane, the viscosity data have been obtained by the correlation given by Huber et al. [17] using density values calculated by the expression given by Cibulka and Hnědkovský [18]. The reported uncertainty for the calculated *n*-decane density and viscosity values is 0.1% and 2%, respectively.

In this work, the densities of ethanol and the binary mixtures are taken from Ref. 8, where they have been measured up to 45 MPa and in the temperature range from 283.15 to 353.15 K for the same compositions considered in this work. The uncertainty reported for these density measurements is 0.1 kg · m^{-3}. For pressures above 45 MPa, the required

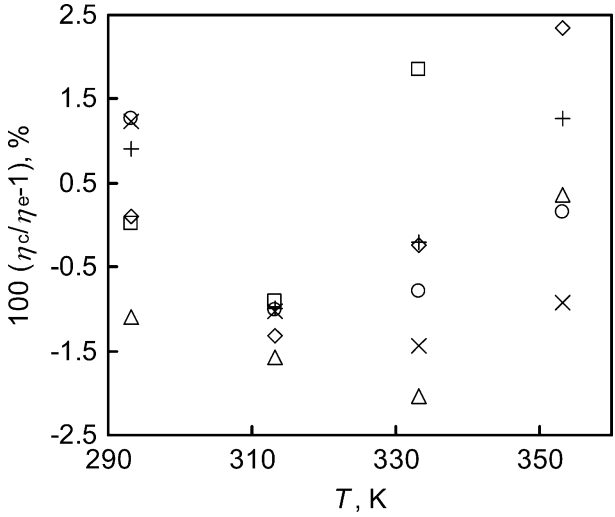

Fig. 1. Comparison of dynamic viscosities for methanol versus the temperature shown as the deviation, $(\eta_c/\eta_e - 1)$, between the calculated values, η_c, by the correlation of Xiang et al. [20] and the experimental values, η_e, of this work: (□) 0.1 MPa, (◇) 20 MPa, (+) 40 MPa, (◯) 60 MPa, (×) 80 MPa, (△) 100 MPa.

densities have been obtained by extrapolation of the experimental densities [8] using the Tait type relation described in Ref. 19.

Taking into account the uncertainty due to the calibration, the temperature, the pressure, and the density, the overall uncertainty for the reported dynamic viscosities is of the order of 2%, found at the highest pressure.

The calibration of the viscometer has been verified by measuring the dynamic viscosity of methanol in the temperature range from 293.15 to 353.15 K at 20 K increments and for pressures up to 100 MPa in steps of 20 MPa. The measured viscosities are reported in Table I as a function of temperature T and pressure P. In Fig. 1, the measured viscosities of methanol are compared with the estimated values obtained by the correlation given by Xiang et al. [20], which is reported to represent the viscosity with an uncertainty less than 2%. Good agreement between the experimental data and the correlation of Xiang et al. [20] is found within the uncertainties reported for the experimental data and the correlated values. The required methanol densities have been obtained by an interpolation of the densities reported by Xiang et al. [20].

At atmospheric pressure (0.1 MPa) the dynamic viscosity has been obtained by measuring the kinematic viscosity, $\nu = \eta/\rho$, with a classical

Table I. Experimental Dynamic Viscosities η for Methanol versus Temperature T and Pressure P

P (MPa)	293.15 K	313.15 K	333.15 K	353.15 K
0.1	0.583	0.445	0.343	
20	0.646	0.497	0.386	0.303
40	0.706	0.546	0.424	0.337
60	0.767	0.593	0.462	0.368
80	0.830	0.640	0.501	0.400
100	0.894	0.683	0.543	0.433

capillary viscometer (Ubbelohde). For this purpose several tubes connected to an automatic AVS350 Schott Geräte Analyzer has been used. The temperature of the fluid is controlled within 0.1 K using a thermostatic bath. When multiplying the kinematic viscosity with the density, the dynamic viscosity is obtained with an uncertainty less than 1%.

The compounds used in this study are commercially available chemicals with the following purity levels: ethanol from Riedel-de-Haën with a chemical purity >99.8 vol.% (Gas Chromatography), a water content <0.2 vol.%, and a molar mass $M_w = 46.07\,g \cdot mol^{-1}$. Toluene was from Aldrich with a chemical purity >99.8% (HPLC Grade) and $M_w = 92.14\,g \cdot mol^{-1}$. *n*-Decane was from Merck with a chemical purity >99% (Gas Chromatography) and $M_w = 142.28\,g \cdot mol^{-1}$. Methanol was from Sigma-Aldrich with a chemical purity >99.93% (HPLC Grade), a water content <0.020%, and $M_w = 32.04\,g \cdot mol^{-1}$. The pure compounds were used as received and stored in hermetically sealed bottles. The binary ethanol (1) + toluene (2) mixtures were prepared immediately before use by weighing at atmospheric pressure and ambient temperature using a high-precision Sartorius balance with an uncertainty of 0.001 g. For each mixture, a sample weighing 250 g was prepared, which, taking into account the uncertainty of the balance, resulted in an uncertainty in the mole fraction of less than 2×10^{-5}.

3. RESULTS AND DISCUSSION

Measurements of the dynamic viscosity have been performed for seven binary mixtures as well as for ethanol (1) and toluene (2) in the temperature range from 293.15 to 353.15 K at 20 K increments and for pressures up to 100 MPa in steps of 20 MPa. The measured viscosities are given in Table II as a function of temperature T, pressure P, and mole fraction of ethanol x_1. However at $T = 353.15$ K and $P = 0.1$ MPa, no

Table II. Experimental Dynamic Viscosities η for Ethanol (1) + Toluene (2) Mixtures versus Temperature T, Pressure P, and Mole Fraction x_1 (for toluene the values are taken from Assael et al. [16])

		$x_1 = 0$	$x_1 = 0.125$	$x_1 = 0.250$	$x_1 = 0.375$	$x_1 = 0.500$	$x_1 = 0.625$	$x_1 = 0.750$	$x_1 = 0.875$	$x_1 = 1$
T (K)	P (MPa)	η(mPa · s)								
293.15	0.1	0.590	0.588	0.609	0.652	0.710	0.790	0.899	1.023	1.194
293.15	20	0.687	0.680	0.710	0.754	0.815	0.909	1.014	1.157	1.344
293.15	40	0.791	0.781	0.816	0.866	0.931	1.034	1.152	1.306	1.494
293.15	60	0.903	0.893	0.931	0.986	1.055	1.166	1.297	1.457	1.647
293.15	80	1.024	1.016	1.054	1.114	1.187	1.302	1.444	1.604	1.797
293.15	100	1.156	1.153	1.189	1.251	1.331	1.449	1.600	1.757	1.955
313.15	0.1	0.469	0.462	0.471	0.490	0.525	0.574	0.635	0.717	0.826
313.15	20	0.546	0.538	0.549	0.573	0.611	0.662	0.729	0.825	0.948
313.15	40	0.628	0.619	0.632	0.658	0.699	0.757	0.830	0.932	1.059
313.15	60	0.715	0.705	0.718	0.747	0.792	0.854	0.933	1.039	1.171
313.15	80	0.807	0.796	0.810	0.841	0.889	0.955	1.038	1.147	1.282
313.15	100	0.906	0.893	0.907	0.940	0.991	1.058	1.145	1.255	1.392
333.15	0.1	0.380	0.370	0.373	0.385	0.405	0.431	0.468	0.523	0.590
333.15	20	0.446	0.433	0.437	0.450	0.470	0.501	0.544	0.603	0.683
333.15	40	0.513	0.499	0.503	0.518	0.540	0.573	0.621	0.684	0.769
333.15	60	0.584	0.568	0.571	0.588	0.611	0.647	0.697	0.763	0.851
333.15	80	0.657	0.639	0.643	0.662	0.686	0.724	0.776	0.844	0.934
333.15	100	0.735	0.714	0.718	0.739	0.763	0.804	0.856	0.926	1.015
353.15	0.1	0.318	0.306							
353.15	20	0.372	0.358	0.356	0.361	0.372	0.390	0.415	0.453	0.510
353.15	40	0.428	0.412	0.411	0.417	0.427	0.446	0.476	0.516	0.574
353.15	60	0.487	0.468	0.467	0.474	0.484	0.504	0.536	0.577	0.636
353.15	80	0.548	0.526	0.525	0.532	0.541	0.564	0.597	0.640	0.699
353.15	100	0.612	0.588	0.586	0.593	0.601	0.625	0.660	0.703	0.763

measurements have been performed for binary mixtures with a concentration of ethanol higher than 25 mol%. The reason is that at these conditions ethanol is a gas and the binary mixtures with a ethanol concentration higher than 25 mol% are located either in the two-phase region or in the vapor state as indicated by the dashed line in the vapor–liquid equilibrium (VLE) phase diagram shown in Fig. 2 for ethanol + toluene along with the reported experimental VLE data [21].

The measured ethanol viscosities have been compared with literature values [6, 22–25], which are available up to 60 MPa in the temperature range from 293.15 to 373.15 K. The literature data have been interpolated in order to obtain values corresponding to the pressures considered in this experimental work. Figure 3 shows the deviations obtained for ethanol viscosities measured in this work as well as the interpolated literature values [6, 22–25], when these viscosity data are compared with the average value obtained by fitting all viscosity values at the corresponding isobar as a function of temperature. This figure shows a very good agreement between the ethanol viscosities of this work and those reported in the literature [6, 22–25].

For all mixtures the viscosity increases with increasing pressure and decreasing temperature. Within the considered *T, P* range, ethanol is the more viscous fluid compared with toluene. With increasing temperature the viscosity of ethanol decreases more rapidly than for toluene, see Table II and Figs. 4 and 5. A quantitative explanation may be due to the weakening or breaking of the formed intermolecular hydrogen bonds

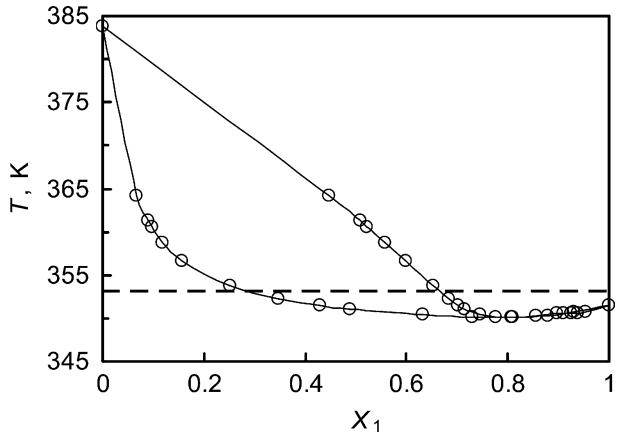

Fig. 2. VLE phase diagram for ethanol (1) + toluene (2) at 0.1 MPa. (◯) experimental data [21] and (– – –) indicates 353.15 K.

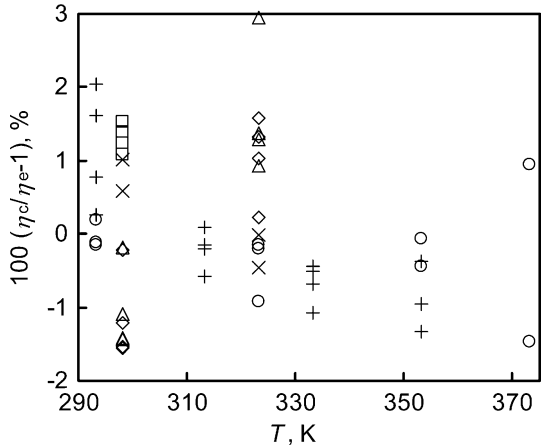

Fig. 3. Comparison of dynamic viscosities for ethanol versus the temperature up to 60 MPa, shown as the deviation, (η_c/η_e-1), between the average fitted values, η_c, obtained from all data (this work and literature [6, 22–25] and the experimental values, η_e,: (+) this work, (□) Papaioannou and Panayiotou [6], (◯) Weber [22], (◇) Tanaka et al. [23], (△) Tanaka et al. [24], (×) Assael and Polimatidou. [25].

(self-association). In Figs. 4 and 5 the variation of the viscosity versus concentration is shown for various isobars at 293.15 and 333.15 K, respectively. A non-monotonic behavior of the viscosity is found for this binary system involving a minimum located near a mole fraction of ethanol $x_1 = 0.125$. This minimum becomes more pronounced with increasing temperature, and also with increasing pressure. It should be mentioned that the experimental data for ethanol + toluene measured by Nikam et al. [26] at 0.1 MPa and at 303.15–308.15 K also reveal a minimum. A minimum in the viscosity behavior versus concentration has also been found for a few other binary systems, for instance, benzene + toluene [27] or 1-methylnaphthalene + 2,2,4,4,6,8,8-heptamethylnonane [28] and the ternary system *n*-tridecane + 1-methylnaphthalene + 2,2,4,4,6,8,8-heptamethylnonane [29]. In Refs. 28 and 29 this behavior has been explained as the result of repulsive interactions. However, a more plausible quantitative explanation for the minimum in the viscosity behavior may be due to the fact that a volume expansion occurs when the two pure compounds are mixed as a result of disruption of the ordered molecular structure within the liquid and a weakening or breaking of the formed hydrogen bonds between ethanol molecules. In Ref. 8, based on the behavior of the experimental

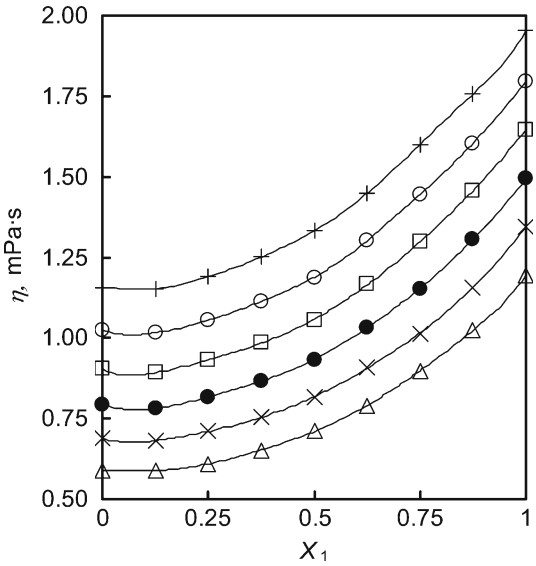

Fig. 4. Dynamic viscosity η for ethanol (1) + toluene (2) versus the mole fraction x_1 at $T = 293.15$ K for (△) 0.1 MPa, (×) 20 MPa, (●) 40 MPa, (□) 60 MPa, (○) 80 MPa, and (+) 100 MPa.

density data and the discussion with respect to the excess molar volume, isothermal compressibility, and isobaric thermal expansivity, it has been found that a volume expansion occurs for this binary system in the toluene-rich region. In the ethanol-rich region, the excess molar volume is negative, but becomes positive with increasing temperature [8]. The negative excess molar volume in Ref. 8 has been interpreted as a result of associative interactions between toluene and ethanol. Despite this and despite the fact that evidence exists for the formation of weak intermolecular associative interactions between aromatic hydrocarbons and alcohols as a result of electron donor–acceptor type of interactions between the π electrons of the aromatic compounds and the hydroxyl group of the alcohol [2–5], no direct effects on the viscosity behavior of the ethanol + toluene binary system are observed, which can be related to these electron donor–acceptor type of interactions. The viscosity behavior of this binary system as a function of the mole fraction shows a negative deviation from ideality.

The excess activation energy of viscous flow ΔE_a can be calculated from the following expression:

$$\ln(\eta_{mix} v_{mix}) = x_1 \ln(\eta_1 v_1) + x_2 \ln(\eta_2 v_2) + \frac{\Delta E_a}{RT}, \tag{2}$$

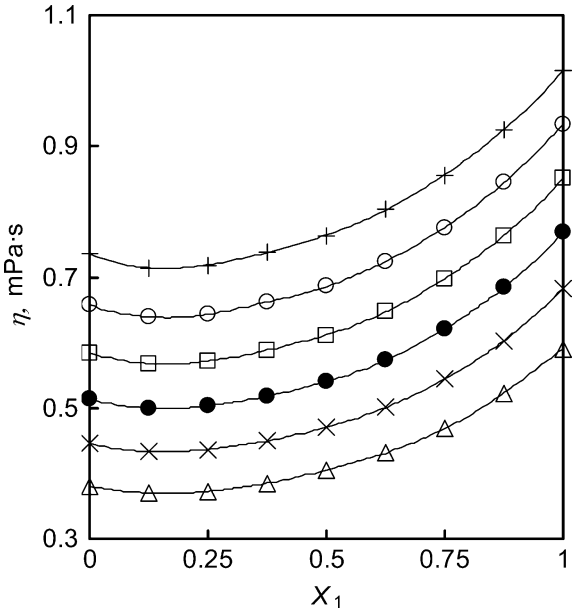

Fig. 5. Dynamic viscosity η for ethanol (1) + toluene (2) versus the mole fraction x_1 at $T = 333.15$ K for (△) 0.1 MPa, (×) 20 MPa, (●) 40 MPa, (□) 60 MPa, (◯) 80 MPa, and (+) 100 MPa.

where R is the universal gas constant and v is the molar volume. Subscript mix refers to the mixture, whereas subscripts 1 and 2 refer to the pure compounds. This relationship is a modified form of the Katti and Chaudhri mixing law [10] and is theoretically justified by Eyring's representation of the dynamic viscosity of a pure fluid [30]. In addition, the quantity ηv is also obtained from the time correlation expression for shear viscosity [31].

The excess activation energy for viscous flow has been calculated using the measured viscosities in Table II and the experimental density data [8] as well as the extrapolated values obtained by the Tait relationship [19]. Within the considered T, P range, the excess activation energy of viscous flow is negative, which corresponds to the fact that the viscosity of the mixtures is reduced compared to that of an ideal mixture, when ethanol and toluene are mixed. The variation of the excess activation energy for viscous flow at 313.15 K is shown as a function of the composition for various isobars in Fig. 6. Similar behaviors are found for the other isotherms considered in this work. Some authors [32–35] have interpreted a negative excess activation energy of viscous flow as the result of the breaking-up of the ordered molecular structure present in the pure liquids and the

fact that repulsive forces or interactions predominate, but it may also be the result of volume expansion. For this binary system, the maximum value of $|\Delta E_a|$ is $335\,J \cdot mol^{-1}$, which corresponds to a weakly interacting system. In comparison, for the binary system methylcyclohexane + 2,2,4,4,6,8,8 heptamethylnonane [36] a maximum value of $700\,J \cdot mol^{-1}$ is found, whereas for a very associative systems, such as water + alcohol [37] the maximum numerical value is $5000\,J \cdot mol^{-1}$. For the ethanol + toluene system $|\Delta E_a|$ decreases with increasing pressure, whereas the changes with temperature are not very pronounced. An explanation may be that when a fluid is compressed the molecular free volume decreases, resulting in molecular interlinking effects and a reduction in their mobility, which consequently leads to a higher viscosity, which corresponds here to a reduction in the absolute value of the excess activation energy for viscous flow as ΔE_a is negative.

For an ideal mixture, $\Delta E_a = 0$, and Eq. (2) becomes the mixing law of Katti and Chaudhri [10]. By comparing the experimental viscosities with the predicted values of Eq. (2), an absolute average deviation (AAD) of 8.0% is obtained with an maximum deviation (MD) = 14% found at $T = 313.15\,K$, $P = 0.1\,MPa$, and $x_1 = 0.375$. The mixing law of Grunberg and Nissan [9];

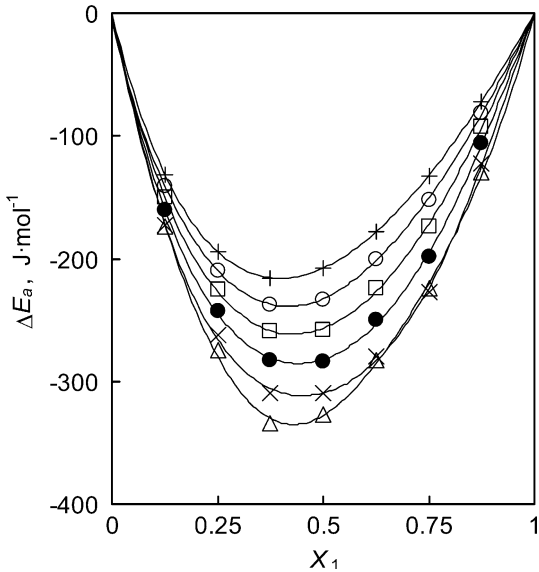

Fig. 6. Excess activation energy for viscous flow ΔE_a for ethanol (1) + toluene (2) versus the mole fraction x_1 at $T = 313.15\,K$ for (Δ) 0.1 MPa, (×) 20 MPa, (●) 40 MPa, (□) 60 MPa, (◯) 80 MPa, and (+) 100 MPa.

$$\ln(\eta_{\text{mix}}) = x_1 \ln(\eta_1) + x_2 \ln(\eta_2) \tag{3}$$

represents the viscosity of the binary mixtures with an AAD of 12% and a MD = 19% found at $T = 313.15$ K, $P = 0.1$ MPa, and $x_1 = 0.500$. By including the molar volume in the Katti and Chaudhri mixing law, it can be seen that the viscosity representation of the binary mixtures is improved compared with the deviations obtained by the Grunberg and Nissan mixing law.

4. CONCLUSION

A total of 209 experimental dynamic viscosity measurements is reported for the ethanol + toluene binary system covering the entire composition range for temperatures between 293.15 and 353.15 K and up to 100 MPa. At 0.1 MPa the dynamic viscosity was measured by a classical capillary viscometer (Ubbelohde) with an experimental uncertainty of 1%, whereas the viscosity under pressure was measured with a falling-body viscometer with an experimental uncertainty of 2%. The calibration of the viscometer was verified by measuring the dynamic viscosity of methanol (23 points) within the same temperature and pressure ranges. For the binary system, the viscosity as a function of composition shows a non-monotonic behavior, with a minimum located around 12.5 mol% ethanol, which can be interpreted as the result of volume expansion. Further, the viscosity behavior of this binary system shows a negative deviation from ideality, which leads to a negative excess activation energy of viscous flow with a maximum absolute value of $335\,\text{J} \cdot \text{mol}^{-1}$, corresponding to a weakly interacting system. The excess activation energy of viscous flow is interpreted as the result of changes in the free-volume, disruption of the ordered molecular structure, and weakening or breaking of hydrogen bonds. The representation of the viscosity of this binary system by the Grunberg and Nissan [9] and the Katti and Chaudhri [10] mixing laws can be considered satisfactory taking into account their simplicity.

ACKNOWLEDGMENT

Financial funding of C.K. Zéberg-Mikkelsen is provided by a Talent project from the Danish Technical Research Council (STVF) Contract No. 26-03-0063.

REFERENCES

1. R. French and P. Malone, *Fluid Phase Equilib*. **228–229**:27 (2005).
2. L. H. Jones and R. M. Badger. *J. Am. Chem. Soc*. **73**:3132 (1951).
3. M. Tamres. *J. Am. Chem. Soc*. **74**:3375 (1952).

4. Y. Ioki, H. Kawana, and K. Nishimoto. *Bull. Chem. Soc. Jpn*. **51**:963 (1978).
5. R. L. Brinkley and R. B. Gupta. *AIChE J*. **47**:948 (2001).
6. D. Papaioannou and C. Panayiotou, *J. Chem. Eng. Data* **39**:463 (1994).
7. U. Sulzner and G. Luft, *Int. J. Thermophys.* **19**:43 (1998).
8. C. K. Zéberg-Mikkelsen, L. Lugo, and J. Fernández, *Fluid Phase Equilib.* **235**:139 (2005).
9. L. Grunberg and A. H. Nissan, *Nature* **164**:799 (1949).
10. P. K. Katti and M. M. Chaudhri, *J. Chem. Eng. Data* **9**:442 (1964).
11. P. Daugé, A. Baylaucq, L. Marlin, and C. Boned, *J. Chem. Eng. Data* **46**:823 (2001).
12. A. S. Pensado, M. J. P. Comuñas, L. Lugo, and J. Fernández, *J. Chem. Eng. Data* **50**:849 (2005).
13. M. C. S. Chen, J. A. Lescarboura, and G. W. Swift, *AIChE J.* **14**:123 (1968).
14. Y. L. Sen and E. Kiran, *J. Supercrit. Fluids.* **3**:91 (1990).
15. E. Kiran and Y. L. Sen, *Int. J. Thermophys*. **13**:411 (1992).
16. M. J. Assael, H. M. T. Avelino, N. K. Dalaouti, J. M. N. A. Fareleira, and K. R. Harris, *Int. J. Thermophys*. **22**:789 (2001).
17. M. L. Huber, A. Laesecke, and H. W. Xiang, *Fluid Phase Equilib*. **224**:263 (2004).
18. I. Cibulka and L. Hnědkovský, *J. Chem. Eng. Data* **41**:657 (1996).
19. A. Et-Tahir, C. Boned, B. Lagourette, and P. Xans, *Int. J. Thermophys.* **16**:1309 (1995).
20. H. W. Xiang, M. L. Huber, and A. Laesecke, submitted to *J. Phys. Chem. Ref. Data*.
21. J. C. Landwehr, S. Yerazunis, and H. H. Steinhauser. *Ind. Eng. Chem. Chem. Eng. Data Ser.* **3**:231 (1958).
22. W. Weber, *Rheol. Acta* **14**:1012 (1975).
23. Y. Tanaka, T. Yamamoto, Y. Satomi, H. Kubota, and T. Makita, *Rev. Phys. Chem. Jpn.* **47**:12 (1977).
24. Y. Tanaka, Y. Matsuda, H. Fujiwara, H. Kubota, and T. Makita, *Int. J. Thermophys.* **8**:147 (1987).
25. M. J. Assael and S. K. Polimatidou, *Int. J. Thermophys*. **15**:95 (1994).
26. P. S. Nikam, B. S. Jagdale, A. B. Sawant, and M. Hasan, *J. Chem. Eng. Data* **45**:559 (2000).
27. J. Zhang and H. Liu, *J. Chem. Ind. Eng. China* **3**:269 (1991).
28. X. Canet, P. Daugé, A. Baylaucq, C. Boned, C. K. Zéberg-Mikkelsen, S. E. Quiñones-Cisneros, and E. H. Stenby, *Int. J. Thermophys.* **22**:1669 (2001).
29. C. K. Zéberg-Mikkelsen, X. Canet, A. Baylaucq, S. E. Quiñones-Cisneros, C. Boned, and E. H. Stenby, *Int. J. Thermophys.* **22**:1691 (2001).
30. S. Glasstone, K. J. Laidler, and H. Eyring, *The Theory of Rate Processes, the Kinetics of Chemical Reactions, Viscosity, Diffusion, and Electrochemical Phenomena* (McGraw-Hill, New York, 1941).
31. R. Zwanzig, *Ann.Rev. Phys. Chem.* **16**:67 (1965).
32. E. L. Heric and J. G. Brewer, *J. Chem. Eng. Data* **22**:574 (1967).
33. I. L. Acevedo, M. A. Postigo, and M. Katz, *Phys. Chem. Liq.* **21**:87 (1990).
34. R. Bravo, M. Pintos, and A. Amigo, *Phys. Chem. Liq.* **22**:245 (1991).
35. P. Cea, C. Lafuente, J. P. Morand, F. M. Royo, and J. S. Urieta, *Phys. Chem. Liq.* **29**:69 (1995).
36. C. K. Zéberg-Mikkelsen, M. Barrouhou, A. Baylaucq, and C. Boned, *High Temp. High Press*. **34**:591 (2002).
37. M. Moha-Ouchane, C. Boned, A. Allal, and M. Benseddik, *Int. J. Thermophys.* **19**:161 (1998).